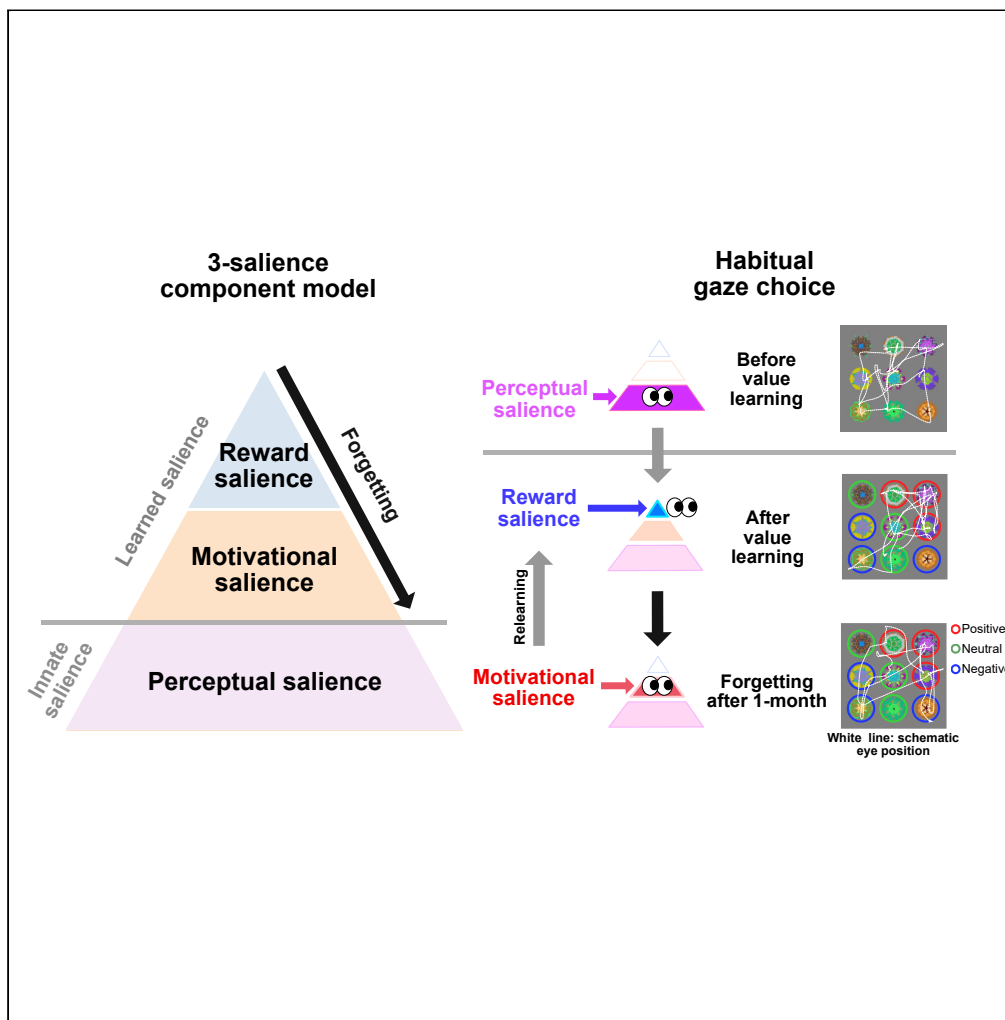


Article

Motivational salience drives habitual gazes during value memory retention and facilitates relearning of forgotten value



Seong-Hwan Hwang, Yongsoo Ra, Somang Paeng, Hyoung F. Kim

hfkim@snu.ac.kr

Highlights

Habitual preference for negatively valued objects emerged during long-term retention

Changes in habitual preference were driven by 3 salience components over time

Preference for negatively valued objects facilitates re-learning of forgotten values

Hwang et al., iScience 25, 105104
October 21, 2022 © 2022 The Authors.
<https://doi.org/10.1016/j.isci.2022.105104>



Article

Motivational salience drives habitual gazes during value memory retention and facilitates relearning of forgotten value

Seong-Hwan Hwang,^{1,2} Yongsoo Ra,^{1,2} Somang Paeng,¹ and Hyoung F. Kim^{1,3,*}

SUMMARY

A habitual gaze is critical to efficiently identify and exploit valuable objects. However, it is unclear what salience components drive the habitual gaze choice. Here, we trained subjects to assign positive, neutral, and negative values to objects and found that motivational salience guided habitual gaze choices over 30 days of memory retention. The habitual preference for negatively valued objects emerged during memory retention. This habitual choice was not explained by a general model with salience components driven by physical features of objects and the rank of learned values. Instead, this is better explained by a model that contains an additional component driven by motivational salience. In a simulated value-forgotten condition, these motivational salience-based habitual choices facilitated re-learning. Our data indicate that after long-term retention, habitual gaze results from increased motivational salience, potentially facilitating the re-learning of forgotten values.

INTRODUCTION

Animals often compete to maximize rewards in the face of limited resources. A strategy for maximizing reward is to find valuable objects associated with the rewards more quickly than other competitors. This first-find, first-earn strategy requires efficient pathways that can quickly and accurately identify valuable objects even when clustered with other objects.

Habitual movement can help to efficiently identify a valuable object (Hikosaka et al., 2013; Land et al., 1999). This behavior can be modified or newly generated by long-term learning of object value. Indeed, habitual movement produces fast and accurate movements with little attentional control that efficiently locates valuable objects (Ghazizadeh et al., 2016a; Kang et al., 2021; Land et al., 1999; Navalpakkam et al., 2010; Yasuda et al., 2012). Primates depend on visual cues, and habitual eye movement is thus a particularly efficient mechanism for making rapid, accurate choices when seeking a valuable object (Kang et al., 2021; Tatler et al., 2011). Imagine a situation where you are walking down the beer aisle. Although you walk into the beer section without much thought, you often quickly identify your favorite brand, allowing you to quickly make a favorite choice. This example shows that habitual eye movement automatically and quickly draws attention to valuable objects.

In primate studies, habitual gaze drawn to highly valued objects is known to be guided by long-term learning of object-value association (Kang et al., 2021; Kim, 2021; Kim and Hikosaka, 2013, 2015; Kim et al., 2015; Yamamoto et al., 2013). When previously learned objects were presented under free-viewing conditions, monkey and human subjects habitually gazed at objects that were previously associated with high reward. This gaze occurred based on learned value association even when a reward was not received in the later free-viewing paradigm.

However, long-term memory, which is the basis of this habitual gaze, is susceptible to forgetting over time (Davis and Zhong, 2017; Ebbinghaus, 1913). Thus, habitual gaze behavior may inevitably be lost by forgetting. However, it is not clear if the habitual gaze behavior is maintained over time or is lost by forgetting. Although forgetting has been investigated in neuroimaging, behavioral, and molecular studies, little is known about how it affects habitual behavior (Davis and Zhong, 2017; Ebbinghaus, 1913; Liu et al., 2016; Oehrns et al., 2018). In addition, forgetting is known to be positively correlated with retention time after

¹School of Biological Sciences, Seoul National University (SNU), Gwanak-ro, Gwanak-gu, Seoul 08826, Republic of Korea

²These authors contributed equally

³Lead contact

*Correspondence: hfkim@snu.ac.kr

<https://doi.org/10.1016/j.isci.2022.105104>



learning, but most studies on habitual behavior were conducted using a limited retention period, making it difficult to demonstrate the effects on longer-term behavioral changes (Averell and Heathcote, 2011; Murre and Dros, 2015; Squire, 1989). It is therefore unclear how changes in long-term value memory occur during the retention period, and how these changes affect habitual preference.

Visual objects have physical features, and some of these are more distinct than others, which causes a difference in perceptual salience (Itti and Koch, 2000). These conspicuous features automatically capture our gazes (Berg et al., 2009; Tatler et al., 2011). However, gaze behavior is affected not only by the exogenous features of objects, but also by previous experiences with objects. These experiences are represented internally in the brain and generate cognitive salience of the experienced objects (Caduff and Timpf, 2008; Schütz et al., 2012; Tatler et al., 2010; Towal et al., 2013). Habitual gaze behavior may be informed by the learned positive, neutral, and negative values of objects (Ghazizadeh et al., 2016a; Kang et al., 2021). Taken together, habitual gaze can be driven by both perceptual and cognitive salience, such as feature salience, learned salience and motivational salience (MS). However, there is still the question of what salience components drive habitual gaze choices during retention time. The link to salience allows us to quantitatively examine the change in contribution of each salience component to habitual gaze choices over time.

To investigate what salience components drive the habitual preference for visual objects over time, human subjects were trained to learn positive, neutral, and negative values of visual fractal objects, and their habitual gazes were examined under free-viewing conditions without outcome after a short and long retention time. In simulated conditions where learned values were forgotten and relearned, we further examined the potential benefit of habitual preference based on MS after long-term retention.

RESULTS

Learning the values associated with visual fractal objects

To examine changes in habitual gaze preference with retention time after learning, we set up an experimental paradigm consisting of two sessions: Learning and Retrieval (Figure 1A). Subjects acquired value information associated with objects during the Learning session. We then tested habitual gaze preference based on value memory in the Retrieval session. During the Learning session, subjects performed an object-value associative learning task in which they learned the positive, neutral, and negative values of visual fractal objects (Figure 1B). Each object was pre-assigned a monetary gain (+¥100; positively valued objects), a monetary loss (-¥100; negatively valued objects), or neither a gain nor a loss (¥0; neutral objects). Subjects were instructed to choose one of two objects by a saccadic eye movement and received monetary feedback following their choice (Figure 1C). The learning task was performed on five consecutive days.

To examine how learning has progressed, we analyzed the percentage of object choice in bins of eight trials (Figure 1D). Subjects showed a gradual increase in choice of positive value objects as learning proceeded, whereas the percentage of times that negative value choices were made decreased (two-way ANOVA with day and bin as factors for the positively valued and negatively valued objects, respectively, $F(1.773, 101.083) = 122.868$, $p = 3.931 \times 10^{-41}$ for day effect of the positively valued objects; $F(1.932, 110.421) = 66.771$, $p = 2.552 \times 10^{-37}$ for day effect of the negatively valued objects) (Figures 1D and S1A). A post-hoc Bonferroni pairwise comparison revealed significant differences in choice performances between the first and the last learning day ($p = 9.9217 \times 10^{-9}$ for positively valued objects, $p = 9.9218 \times 10^{-9}$ for negatively valued objects). In addition, on the last day of learning, subjects showed significant differences between choice percentage of valued objects (one-way ANOVA with value as factor; $F(2, 1389) = 1725.97$, $p = 2.2 \times 10^{-16}$ for value effect). These results indicate that value memory for objects was successfully acquired during the 5-day learning period.

To further confirm whether subjects can explicitly remember the values of fractal objects after the Learning session, subjects were tested for explicit memory after a retention period of one day and more than 30 days (Day >30). For each trial in the explicit memory task, subjects were presented with a learned or novel object and instructed to choose an answer for learned values and novelty of objects with a keyboard (Figure 1E). After a 1-day retention period, the percentage choice of objects where the value was correctly assigned was higher than chance in the explicit memory test (Positive value: 97%, Neutral: 79%, Negative value: 88%) (Right-tailed binomial test, $p = 9.813 \times 10^{-166}$, $p = 1.716 \times 10^{-97}$, and $p = 8.623 \times 10^{-129}$ for positively, neutral and negatively valued objects, respectively), indicating that the subjects were able to explicitly retrieve the memory of the objects (Figure 1F, left panel). The memory of object values was retained

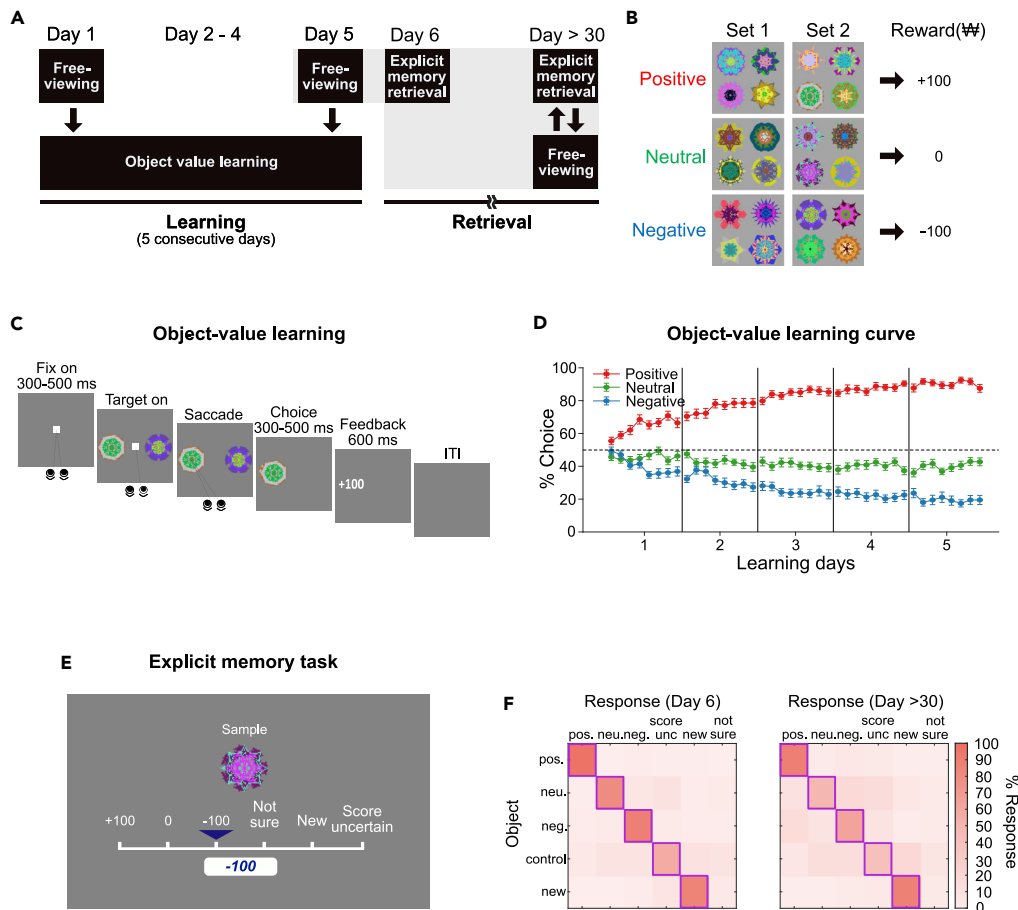


Figure 1. Overall experimental design, object-value learning task and explicit memory task

(A) The experiment consisted of Learning and Retrieval sessions. The Learning session was conducted for 5 consecutive days to associate values with objects. In the Retrieval session, the explicit memory task and free-viewing condition were conducted.

(B) Example set of fractal objects. During the object-value learning task, the subjects were trained to associate fractal objects with monetary gain (positively valued: +¥100), monetary loss (negatively valued: -¥100), or neither a gain nor a loss (neutral: ¥0).

(C) Object-value learning task. During each trial of the object-value learning task, subjects were instructed to choose one of two fractal objects by making a saccadic eye movement. After choosing an object, the associated outcome was shown on the screen.

(D) Learning curve of object-value learning task. Each graph shows a learning curve for percentage choice data analyzed in bins of eight trials. There was an increase in the ratio of choosing positively valued objects as learning proceeded, while the ratio of choosing negatively valued objects decreased. Error bars indicate between-subject standard error ($n = 29$ subjects, two sets of eight objects for each subject: 58 individual data points for each value).

(E) Explicit memory task. One object among the learned and novel fractal objects was presented, and the participants were asked to choose one of six possible answers.

(F) Percentages of responses in the explicit memory task on Day 6 and Day >30. Correct answers for each response are indicated with purple boxes (pos.: positive, neu.: neutral, neg.: negative, score unc.: score uncertain).

more than 30 days after the initial learning session: the percentage of correct value assignments for positively, neutral, and negatively valued objects was significantly higher than chance (Positive value: 88%, Neutral: 49%, Negative value: 63%) (Right-tailed binomial test, $p = 8.623 \times 10^{-129}$, $p = 3.956 \times 10^{-30}$, and $p = 7.567 \times 10^{-57}$ for positively, neutral and negatively valued objects, respectively) (Figure 1F, right panel).

Habitual gaze preference toward positively valued objects one day after long-term learning

Next, to investigate how the habitual gaze preference changes over time, automatic eye movements (saccades) were examined under free-viewing conditions before the learning session (Pre-learning), one day

after four-day learning (Day 5), and more than 30 days after the final learning session (Day >30). Under free-viewing conditions, nine out of 12 learned objects were pseudo-randomly chosen for each trial and presented as a three-by-three array on the screen for 8 s without any reward outcome (total 16 trials/session) (Figure 2A). This procedure allowed measurement of automatic gaze in subjects in the absence of an immediate goal or purpose.

We measured the number of first and overall gazes as well as fixation time on learned objects. On Day 5, we found significant differences in the number of first gazes when comparing learned objects by value group (one-way ANOVA, $F(2,171) = 15.02$, $p = 9.7 \times 10^{-7}$ for value) (Figure 2C). A post-hoc Bonferroni pairwise comparison revealed that the first gazes to positively valued objects were significantly more frequent compared to neutral and negatively valued objects ($p = 5.4 \times 10^{-6}$ for positively valued and neutral objects; $p = 7.0 \times 10^{-6}$ for positively valued and negatively valued objects). In addition, the number of gazes and fixation time were significantly different between value groups of the learned objects (one-way ANOVA, $F(2,171) = 32.05$, $p = 1.5 \times 10^{-12}$ for value in number of gazes; one-way ANOVA, $F(2,171) = 4.43$, $p = 0.013$ for value in stay time per fixation) (Figures 2B and 2C). A post-hoc Bonferroni pairwise comparison revealed a higher number of gazes toward objects with positive value than neutral and negatively valued objects ($p = 9.5 \times 10^{-10}$ for positively valued and neutral objects; $p = 1.0 \times 10^{-9}$ for positively and negatively valued objects) and more stay time on positively valued objects than neutral and negatively valued objects ($p = 0.024$ for positively valued and neutral objects; $p = 0.029$ for positively and negatively valued objects). However, there were no significant differences in habitual gaze preference between neutral and negatively valued objects on Day 5 ($p = 0.990$ for the first gaze; $p = 0.838$ for number of gazes; $p = 0.998$ for stay time per fixation). Our data reveal that long-term learning of object-value association generates a habitual gaze preference for objects previously associated with a positive reward.

Because participants were instructed to choose the higher-valued objects in our learning task, they were inevitably more exposed to higher-valued objects as learning proceeded. This may result in a preference for familiar objects (mere-exposure effect) (Park et al., 2010; Zajonc, 2001). To eliminate this possibility, we conducted a control learning task in which fractal objects were presented with different levels of frequencies (high, low, and no exposure during control learning task). We found no significant differences in gaze behavior toward each exposure group of the objects under free-viewing conditions on Day 5 and Day >30 (Figure S2). These results indicate that the habitual gaze preference is not due to differences in familiarity.

Selective increase in habitual gaze to negatively valued objects after longer retention

We next tested whether habitual gaze preference is sustained more than 30 days after the last learning session. We found significant differences in the number of first gazes when comparing learned objects by value group (one-way ANOVA, $F(2,171) = 15.16$, $p = 8.7 \times 10^{-7}$) (Figure 2C, left panel). A post-hoc Bonferroni pairwise comparison showed that the first gaze to positively valued objects was significantly greater than that to neutral and negatively valued objects after more than 30 days of retention time ($p = 1.1 \times 10^{-7}$ for positively valued and neutral objects; $p = 0.025$ for positively valued and negatively valued objects). Additional analyses found significant differences in both the number of gazes and fixation duration time when comparing value groups (one-way ANOVA, $F(2,171) = 26.34$, $p = 1.0 \times 10^{-10}$ in number of gazes, $F(2,171) = 3.74$, $p = 0.025$ in stay time per fixation) (Figure 2C, middle and right panels). The number of gazes and duration of fixation on positively valued objects was also significantly greater compared to neutral and negatively valued objects ($p = 9.5 \times 10^{-10}$ and $p = 2.6 \times 10^{-5}$ compared with number of gazes on neutral and negatively valued objects, respectively; $p = 1.7 \times 10^{-2}$ compared with stay time per fixation to neutral objects). Taken together, the habitual gaze preference for positively valued objects observed on the last day of learning was maintained more than a month later.

Although participants maintained a habitual gaze preference for positively valued objects, the preference for negatively valued objects selectively changed after 30 days of retention. Participants developed a stronger preference for negatively valued objects over neutral objects after a long retention time: the number of first and overall gazes to negatively valued objects were significantly higher compared to those to neutral objects on Day >30 (two-tailed unpaired t-test, $p = 0.01$ for the first gaze and $p = 0.016$ for the number of gazes) (Figure 2C).

To quantify this negatively valued object-selective increase in habitual gaze behavior, we examined the individual rate of change in the number of first gazes, number of gazes, and fixation duration time from Day 5 to Day >30 (Figures 2D and S1B). Of interest, the habitual gazes to negatively valued objects selectively

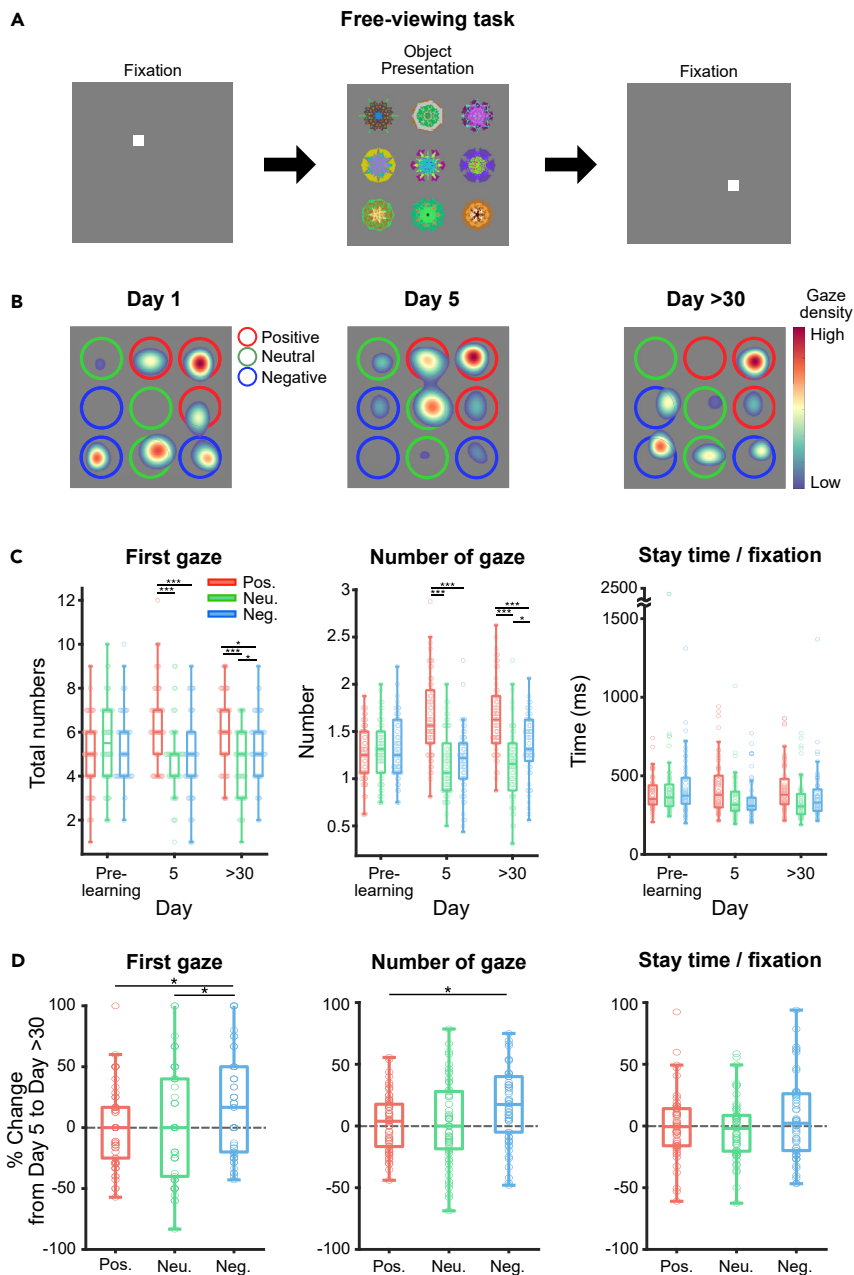


Figure 2. Scheme of free-viewing task and habitual gaze changed after long retention times

(A) Free-viewing condition. During each trial in the free-viewing condition, a fixation dot was followed by the fractal objects. The subjects were instructed to freely view the nine fractal objects without any feedback.

(B) Example heat maps showing the fixation density of a subject on Day 1, 5, and >30. The colored circles around the fractal objects indicate the learned values of each fractal object (red: positively valued, green: neutral, blue: negatively valued). Learned values and gaze density are respectively indicated by colored circles and a heatmap without fractal objects to aid clear visualization; fractal objects were presented in the free-viewing task.

(C) Box-and-whisker plots with individual points for three gaze properties during the free-viewing condition for pre-learning and after-learning periods ($n = 58$).

(D) The percentage change of individual subjects in three gaze properties from Day 5 to Day >30 ($n = 58$). * $p < 0.05$, *** $p < 0.001$.

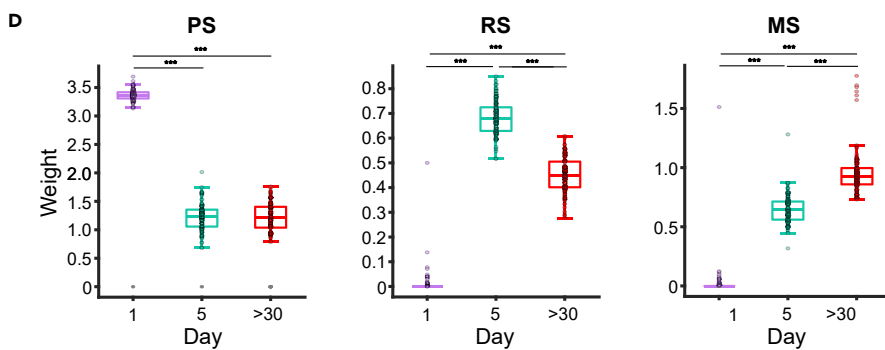
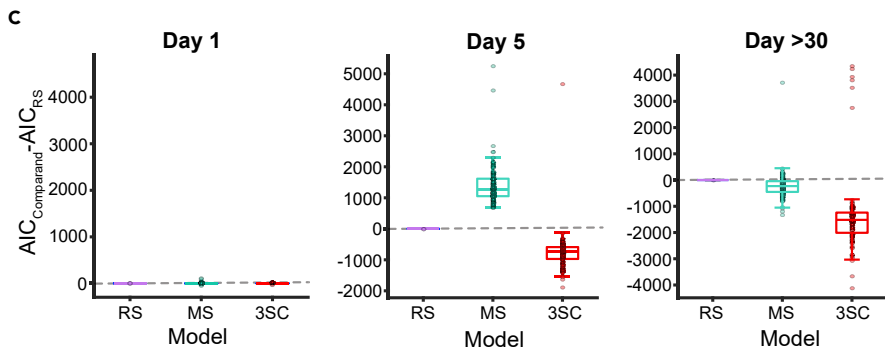
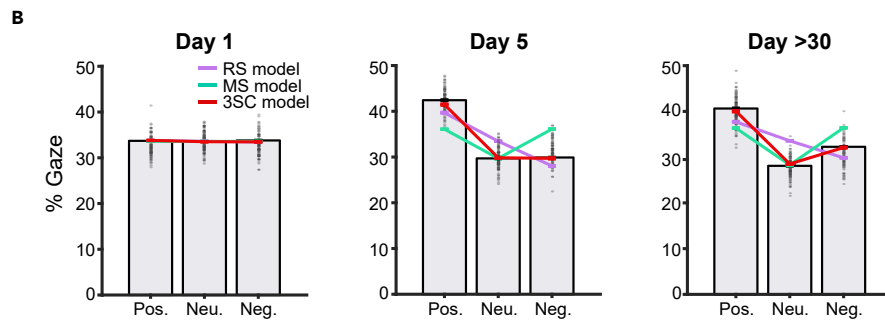
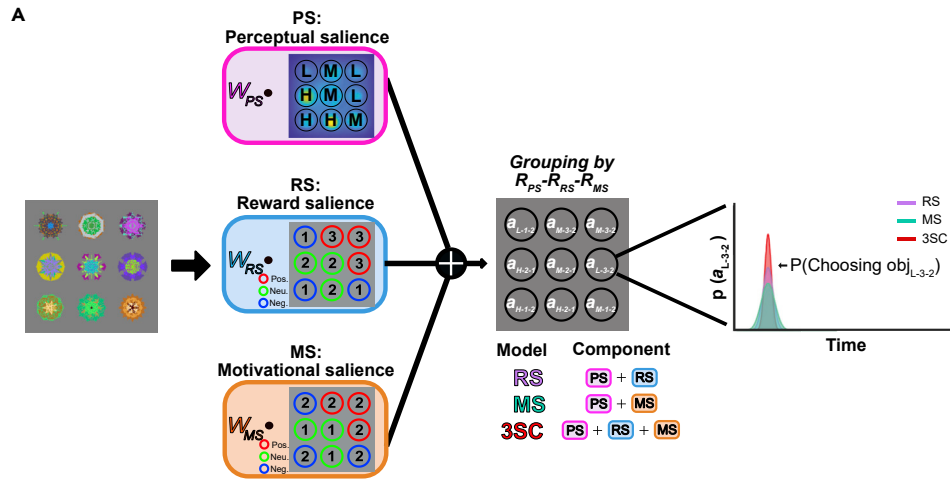


Figure 3. Model schematics and comparison between modeled gaze and actual gaze

(A) Model fitting procedure. The nine objects were split into three predictors of PS, RS and MS, and ranked in two levels for MS or three levels for PS and RS. The rank tuples were used to categorize the objects, and the frequency of choosing each category across all trials was fitted by the three weights multiplied by each predictor.

(B) Modeled gaze versus actual gaze. Bar graphs show the proportions of each value-learned object being gazed at. The colored lines represent predictions from the three models. Gray bars indicate the percentages of habitual gaze in the free-viewing condition. Black dots represent individual bootstrapped data points for percentages of habitual gaze in the free-viewing condition.

(C) The best model for habitual gaze after short-term and long-term retention times. Each model on Day 1, 5 and >30 was compared to the AIC value for the RS model. The AIC values of MS and 3SC models were subtracted from the AIC value of RS model.

(D) Changes in weights on PS, RS, and MS components across days. Box-and-whisker plots show weights on PS, RS and MS components in the 3-SC model across days. *** $p < 0.001$.

changed after long-term retention: the change rates in numbers of the first and overall gaze to negatively valued objects were significantly greater than those to positively valued and neutral objects (one-way ANOVA, $F(2,171) = 4.96$, $p = 0.008$ in the first gaze, and $F(2,171) = 4.09$, $p = 0.018$ in the overall gaze). Post-hoc Bonferroni pairwise comparison revealed significant differences between negative value and other values in both properties ($p = 0.008$ for positively valued and negatively valued objects, $p = 0.04$ for neutral and negatively valued objects in the first gaze. $p = 0.02$ for positively valued and negatively valued objects in the number of gazes) (Figure 2D). Taken together, habitual gaze preference for negatively valued objects was selectively increased in long-term retention.

A computational model including the motivational salience component explains the change in habitual gaze preference over time

Next, we investigated what components might guide the change of habitual gaze over time. The graph-based visual saliency method (GBVS) with perceptual salience (PS) can predict the innate gaze bias of human participants from low-level visual features (Harel et al., 2007; Kumar et al., 2019). During free-viewing conditions, the innate gaze bias to presented objects before learning was successfully predicted using the GBVS method (Figure S3A). After object-value associative learning, we expected that the habitual gaze under free-viewing conditions was driven by learned values of objects as well as innate gaze preference. We thus introduced reward salience (RS) to the GBVS model, which is referred to as the RS model consisting of PS and RS (Figure 3A). However, the RS model did not explain either the number of habitual gazes on Day 5 or on Day >30 (Figure 3B). Our data indicate that two types of saliences, PS and RS, were insufficient to guide the observed habitual gaze behavior after both short-term and long-term retention, suggesting that another component may be required.

What component might plausibly predict this habitual gaze preference? Previous studies reported that memory of the highest and lowest values is better retrieved than that of the intermediate ones (Ghazizadeh et al., 2016b; Madan, 2013; Madan and Spetch, 2012). They suggested that salience can be defined by a quadratic relationship with value, such that the highest (by monetary gain or reward) and lowest (by monetary loss or aversion) values are higher in salience than the neutral value, referred to as MS (Madan, 2013; Madan and Spetch, 2012; Ventura et al., 2007). Furthermore, a single dopamine neuron in the primate brain showed higher responses to positive and negative values than neutral value, suggesting the brain process of MS (Matsumoto and Hikosaka, 2009). We thus hypothesized that this salience on the positive and negative values of learned objects is reflected in habitual gaze behavior. To test this idea using a habitual gaze prediction model, we introduced this MS component into the previous RS model, in which the highest rank was assigned to positively valued and negatively valued objects, (3-salience component model (3SC)) (Figure 3A). Notably, this new model with PS, RS, and MS successfully predicted the percentage of habitual gaze preference toward each value group of objects on both Day 5 and Day >30 (Figures 3B and S4C). However, a model with only PS and MS (MS model) still could not explain the gaze number (Figures 3B, S4A, and S4B).

To quantitatively examine the best-fit model, we next compared the Akaike information criterion (AIC) values of the MS and 3SC models to that of the RS model (Figure 3C). The subtracted values between the AIC values of RS and 3SC models were lower than other subtracted values on Day 5 and Day >30, but not on Day 1 (one-way ANOVA, $F(2,297) = 125.14$, $p = 3.8 \times 10^{-40}$ for models on Day 5; one-way ANOVA, $F(2,297) = 31.9$, $p = 2.8 \times 10^{-13}$ for models on Day >30) (Figure 3C). A post-hoc Bonferroni pairwise comparison test confirmed the statistical differences between the subtracted AIC values ($p < 4.9 \times 10^{-7}$ and

$p < 3.2 \times 10^{-12}$ for 3SC and RS models on Day 5 and Day >30, respectively; $p = 6.6 \times 10^{-40}$ and $p = 4.6 \times 10^{-9}$ for 3SC and MS models on Day 5 and Day >30, respectively). These results reveal that the MS component is essential to explain not only the habitual gaze preference after a short retention time but also its change after long-term retention. We also tested an alternative 3SC model consisting of PS, RS, and variants of MS and found that the 3SC model with MS explains the data better than the one with alternatives, suggesting that the explanatory power of the 3SC model is due specifically to the MS component (Figure S3B). Taken together, our 3-salience component model demonstrates that habitual gaze preference after long-term learning is guided by reward value salience and MS, in addition to innate PS.

Increase in motivational salience effects on habitual preference with retention time

To further examine the relative contribution of each salience component to the 3SC model (the best-fit model), we calculated the weight contributed by three free parameters, PS, RS, and MS (Figure 3D). PS weight decreased after learning (one-way ANOVA, $F(2,297) = 7390.312$, $p = 5.2 \times 10^{-254}$; post-hoc Bonferroni pairwise comparison, $p < 1.5 \times 10^{-133}$ and $p < 6.7 \times 10^{-136}$ for the weight values for PS before learning compared to the weight on Day 5 and to on Day >30, respectively). In contrast, both weight values for RS and MS increased after learning (one-way ANOVA, $F(2,297) = 2717.291$, $p < 1.3 \times 10^{-191}$ for RS; one-way ANOVA, $F(2,297) = 868.872$, $p < 7.9 \times 10^{-125}$ for MS) (Figure 3D, middle and right panels). Significant differences among the PS, RS, and MS weights were observed after learning (one-way ANOVA, $F(2,297) = 331.46$, $p < 2.2 \times 10^{-76}$ on day 5; one-way ANOVA, $F(2,297) = 868.872$, $p < 7.9 \times 10^{-125}$ on Day >30). A post-hoc Bonferroni pairwise comparison test confirmed that the weight value for PS was greater than the weight values for RS and MS on Day 5 ($p < 1.5 \times 10^{-62} \times 10^{-10}$ for RS and $p < 4.3 \times 10^{-67}$ for MS) and Day >30 ($p < 1.0 \times 10^{-57}$ for RS and $p < 6.3 \times 10^{-8}$ for MS), suggesting that habitual gaze was still affected by PS even after learning (Figure 3D, left panel).

Of interest, the values of RS and MS weights changed in opposite directions during the post-learning retention period (Figure 3D, middle and right panels). The weight value for RS increased one day after value learning, then decreased in retention periods >30 days (a post-hoc Bonferroni pairwise comparison, $p = 6.5 \times 10^{-75}$ between the RS weights on Day 5 and Day >30) (Figure 3D middle panel). However, the increased weight value for MS one day after learning showed a greater increase after long-term retention without additional learning (a post-hoc Bonferroni pairwise comparison, $p < 4.9 \times 10^{-33}$ between the MS weights on Day 5 and Day >30) (Figure 3D, right panel). These data show that the major salience components that drive habitual gaze preference change with longer retention times from reward value salience to MS.

Motivational salience indicates that forgetting drives changes in habitual gaze preference

In our data, the contribution of salience driven by reward value memory (RS) decreased more than 30 days after the last learning session (Figure 3D, middle panel). It is known that memory degrades over time, and this forgetting may lead to the observed dynamic changes in the contribution of salience components (Ebbinghaus, 1913; Graybiel, 2008). We therefore hypothesized that participants who forget more about the learned value may show fewer RS-based habitual gazes, instead of gaze being based on the other salience component, MS.

To test this hypothesis, we first divided the boot-strapped samples into two groups: those that fit the RS model better than the MS model (RS group), and vice versa (MS group). The extent of forgetting the learned values was calculated with the percent decrease in the correct answer rate from one day (Day 6) to more than 30 days (Day >30) after learning in the explicit memory test (explicit forgetting index). We then compared the forgetting indices between RS and MS groups. There were no significant differences in explicit task performance for the RS and MS groups on Day 6 and Day >30 (Figure S3C). The MS group achieved slightly greater performance than RS group on day 6, whereas the RS group achieved slightly greater performance than MS group on day 30, although the differences were not statistically significant. After the subtraction of individual indices, however, this difference resulted in a significantly different forgetting index. We found that the forgetting index in the MS group was significantly, albeit weakly, greater than the RS group (two-tailed unpaired t-test, $p < 2.2 \times 10^{-2}$, $n = 36$ and $n = 64$, boot-strapped samples, for RS and MS groups, respectively) (Figure 4A). This suggests that participants with a greater extent of forgetting, rather than learning performance, have habitual gaze behavior that is driven more by MS than RS.

Next, we examined the correlation between the explicit forgetting index and the index for the preferred model. Since a lower AIC value means better fit to the observed data, the negative correlation in Figure 4B

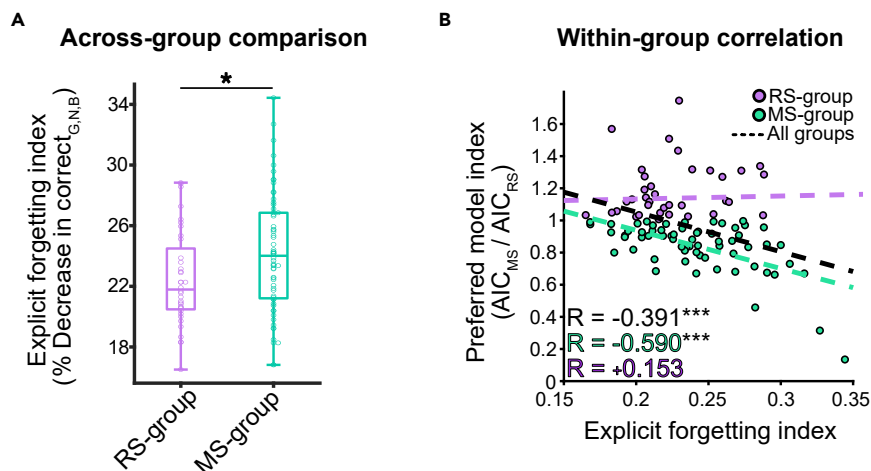


Figure 4. More forgetting of object values leads to a habitual gaze that is based on motivational salience

(A) Comparison of forgetting index from an explicit task between a group better fitted by the RS model (RS group) and a group better fitted by the MS model (MS group).

(B) Relationship between the preferred model and the degree of forgetting. Purple and green dots indicate the RS group and the MS group, respectively ($n = 100$ bootstrapped samples). Purple, green, and black dotted lines represent a linear fit to RS group, MS group and all samples, respectively. Because the lower index of the preferred model indicates a better fit to the MS model, the negative correlation shows that the MS model predicts the habitual gaze better than the RS model when participants experienced a greater extent of forgetting. * $p < 0.05$, *** $p < 0.001$.

indicates that the subjects who forgot more about the learned values had habitual eye gazes that were driven by MS ($r = -0.39$, $p < 5.3 \times 10^{-5}$, Pearson correlation). This negative correlation was more prominent with the indices of subjects in the MS group ($r = -0.590$, $p < 2.8 \times 10^{-7}$, Pearson correlation) (Figure 4B). However, there was no significant correlation in the RS group ($r = 0.153$, $p < 3.75 \times 10^{-1}$). Together, these results suggest that greater forgetting of learned object values results in the habitual gaze being more dependent on MS after a long retention period.

Efficient motivational salience-based re-learning strategy through habitual gaze preference after forgetting

What is the functional advantage of habitual search guided by MS? Greater forgetting of object values induced more MS-guided habitual gazes. We therefore tested whether the MS-guided habitual search might be an efficient re-learning strategy after forgetting.

To investigate the functional advantage of MS-guided habitual search, we designed a paradigm that simulated learning, forgetting, and re-learning with three objects each associated with different mean reward values (-epsilon, 0, and +epsilon) (Figure 5A). During the learning phase, objects were freely chosen based on prior experience (prior probability in a Bayesian model). The value of the chosen objects was then revealed. The likelihood function based on the value of the chosen object was used for computing posterior belief over the object's mean reward distribution. The SD of posterior belief after the learning phase was added by a forgetting factor, F , to simulate forgetting. In the re-learning phase, the reward gain based on the updated posterior from four different choice strategies was examined. Two of the four strategies were based on our previous model components: MS-guided choice strategy (2:1:2 for positively valued, neutral, and negatively valued objects) and RS-guided choice strategy (3:2:1). We also added two additional alternative strategies (2:2:1 and 1:2:2) to the simulation. We first tested these strategies in situations where the values were completely forgotten (Figures 5A and 5B). The rates at which reward gain increases under the four strategies were significantly different (one-way ANOVA, $F(3,396) = 95.22$, $p < 2.045 \times 10^{-464}$ for comparing exponentials in a log-fitted curve to regard gain across re-learning steps) (Figure 5B). Notably, the post-hoc Bonferroni pairwise comparison revealed that reward gain through MS-guided choice (2:1:2; positively and negatively valued objects are chosen more than neutral objects) exponentially increased at a greater rate than that by the other three strategies ($p < 6.099 \times 10^{-36}$, $p < 1.918 \times 10^{-28}$, and $p < 2.017 \times 10^{-38}$ for comparing to 2:2:1, 1:2:2, and 3:2:1 strategies, respectively). There were no significant differences among the remaining three strategies. To further examine the step at which this difference

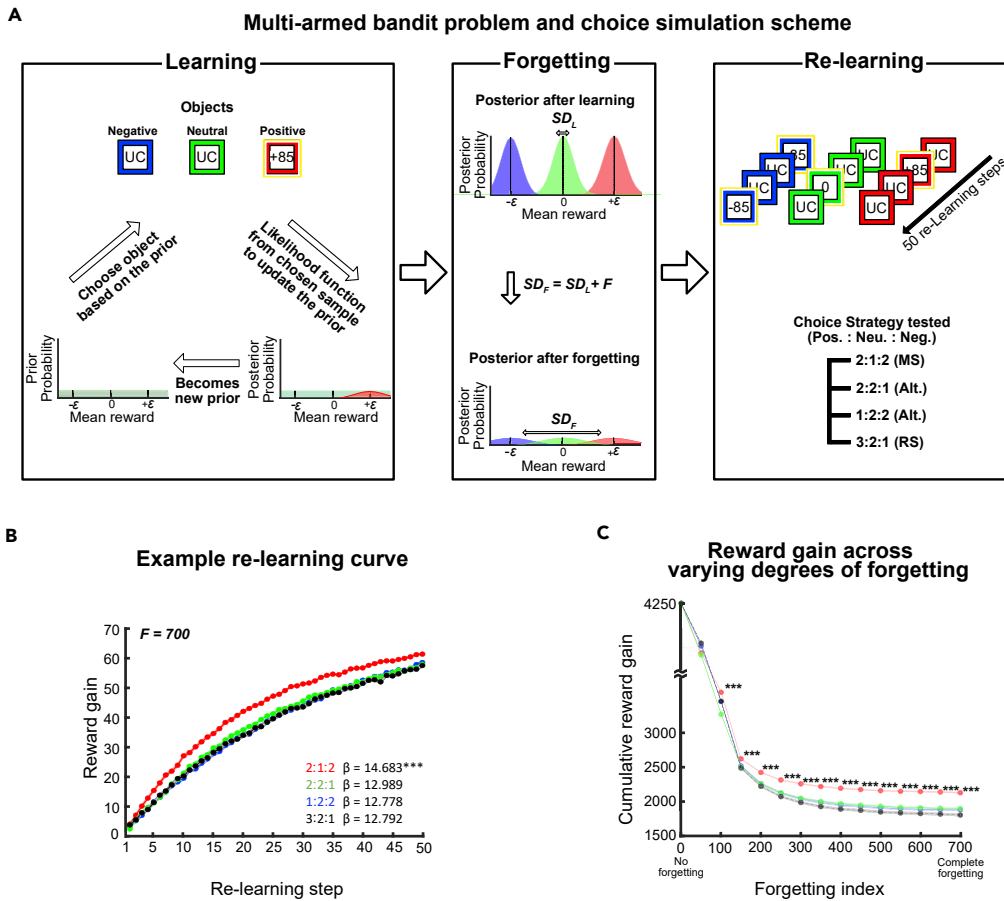


Figure 5. Behavioral simulation of re-learning under Bayesian framework

(A) Simulation scheme for learning, forgetting, and re-learning. Three objects consisted of negatively valued, neutral, and positively valued objects with means of $-\epsilon$, 0 and $+\epsilon$. The simulation consists of three phases: Learning, forgetting, and re-learning. Object values were chosen based on the prior, and the prior was updated by likelihood function obtained from a chosen object. UC denotes unchosen objects, whereas objects with values represent chosen objects, whose values are being revealed. We increased the standard deviation (SD) of prior over the mean of each object to simulate the effect of forgetting. Four different choice strategies were examined, and we let the observer stochastically chose one of the three objects. For each re-learning step, the value of the chosen object is revealed, which is used to update the observer's posterior distribution. The mean reward gain was calculated for each step to assess the functional benefit of different choice strategies.

(B) Re-learning curve across 50 re-learning steps under complete forgetting, whereby the high-valued objects are selected at a chance level (Forgetting factor (F) = 700).

(C) Comparison of reward gains accumulated during the 50 re-learning steps at varying degrees of forgetting. 2:1:2 (MS-driven gaze choice), 3:2:1 (RS-driven gaze choice), 2:2:1, and 1:2:2 denote the ratios of the choice between positively valued, neutral, and negatively valued. The 2:2:1 and 1:2:2 strategies were tested as alternatives to the 2:1:2 strategy. $***p < 0.001$.

arises, we directly compared the reward gain from the four strategies. We observed significant differences among the four strategies in their reward gains starting from re-learning step 2 (one-way ANOVA, $F(3,396) = 3.43$, $p < 1.710 \times 10^{-2}$). Bonferroni pairwise comparison further revealed that MS-guided habitual gaze attains significantly different reward gain than all three other strategies at re-learning step 3 ($p < 2.966 \times 10^{-5}$, $p < 6.463 \times 10^{-3}$, and $p < 4.731 \times 10^{-3}$ for comparing to 2:2:1, 1:2:2, and 3:2:1 strategies, respectively) (Figure 5B). Thus, these results demonstrate that MS-guided habitual gaze results in a functional advantage compared to other strategies early in their re-learning.

To investigate whether the MS-guided choice strategy is best for identifying valued objects in different states of forgetting, cumulative reward gains were calculated during re-learning with different degrees

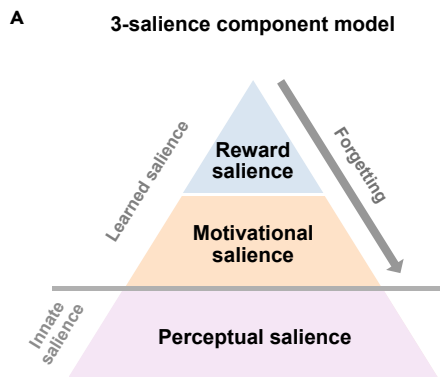


Figure 6. The 3-salience component model

(A) Innate salience on low-level features (perceptual salience) mainly guides habitual gaze behavior before object-value learning. In contrast, after learning, the learned salience components, RS and MS, contribute to the habitual gaze. The contributions of RS and MS to the habitual gaze decrease and increase, respectively, under forgetting, whereas that of PS is relatively intact.

of forgetting (Figures 5C and S5). We found significant differences among the reward gains achieved by the four strategies when the forgetting index was at 100 and above (one-way ANOVA, $F(3,396) = 54.84$, $p < 1.148 \times 10^{-29}$ for Forgetting index = 100) (Figure 5C). A post-hoc Bonferroni pairwise comparison revealed significant differences between the reward gain with MS-guided choice strategy and the gains with all other strategies ($p < 5.591 \times 10^{-6}$, $p < 1.194 \times 10^{-29}$, and $p < 1.110 \times 10^{-3}$ for comparing to 2:2:1, 1:2:2, and 3:2:1 strategies, respectively). We confirmed that this difference persisted when the forgetting index was greater than 100. In contrast, when the forgetting index is 50, we found that simulated choices with the RS-guided (3:2:1) or 2:2:1 strategy resulted in the greatest reward gain compared to MS-guided (2:1:2) or 1:2:2 strategies. This result suggests that RS-guided choice maximizes the reward gained when memory is relatively intact (one-way ANOVA, $F(3,396) = 127.35$, $p < 9.383 \times 10^{-58}$ for Forgetting index = 50) (Figure 5C). A post-hoc Bonferroni pairwise comparison revealed that choices with 3:2:1 and 2:2:1 result in significantly greater reward than 1:2:2 or 2:1:2, but there were no significant differences between 3:2:1 and 2:2:1 strategies (3:2:1 strategy: $p < 8.028 \times 10^{-39}$, and $p < 5.081 \times 10^{-35}$, compared to 1:2:2 and 2:1:2, respectively; 2:2:1 strategy: $p < 1.314 \times 10^{-34}$, and 6.676×10^{-31} for 2:2:1, comparing to 1:2:2 and 2:1:2, respectively). Thus, our simulation results show that when value memory is degraded, habitual choice based on MS helps the subject to strategically re-learn the forgotten values of fractal objects to maximize reward gain.

DISCUSSION

We have demonstrated how habitual gaze preference changes during memory retention period. A month after learning, gaze preference for positively valued objects changes into a preference for both positively valued and negatively valued objects, but not neutral objects. This change in gaze preference is best explained by dynamic changes in the reward value salience (RS) and MS across time. We observed that the goodness-of-fit of MS model to habitual gaze behavior increased while that of RS decreased, depending on the extent of forgetting. Our follow-up simulation further showed that the change in salience contribution supports re-learning of object values after forgetting, thus maximizing reward given a limited exploration time.

3-Salience component model to guide habitual preference: Implications for learning and different rates of forgetting

We suggest a 3-salience component model in which the contribution of each salience component changes to control the habitual gaze in different phases of learning and retention. Before learning of object value, habitual gaze is primarily guided by PS favoring low-level features such as colors, shapes, and sizes. In the days following learning sessions the salience components RS and MS drive habitual gaze behavior together with PS (3-salience component model) (Figure 6). The changes in weights of salience components support this model. Before learning, the PS weight was significantly above 0, but others were not (Figure 3D), indicating that PS mainly contributes to guide habitual gaze behavior. After learning, the contribution of PS decreased, but the weights of RS and MS increased. This suggests that learned salience components take part in driving our habitual gaze after learning.

Furthermore, habitual gaze behavior after a retention period of one month shows that the contribution of each salience component changes at a different rate over time. The contributions of the RS and MS

components to habitual gaze changed in opposite directions after a long retention period: the RS contribution decreased, whereas the MS contribution increased (Figure 3D). However, the contribution of PS to gaze behavior was sustained after long-term retention.

These changes in the contribution of salience components indicate that some components are more susceptible to forgetting than others. During the long-term retention period, learned salience components could decay at different speeds. The most likely explanation for our data is that RS fades much faster than MS across retention time. This suggests a sequential forgetting model where salience components decay sequentially from RS to MS (Figure 6). With this successive forgetting, habitual gaze behavior is guided mainly by a remaining salience component. Indeed, we found that habitual gazes of participants who showed more forgetting of object values were guided by MS rather than RS (Figure 4).

The origin of motivational salience

An obvious next question is what generates MS, given that it is such an important component of habitual gaze behavior. Previous studies suggest that emotional valence might drive MS linked to habitual gaze (Costanzi et al., 2019; Lang et al., 1998; Ohgami et al., 2006; Russell, 1980). For example, gain and loss of the monetary reward also increases the positive and negative valence levels of emotion, respectively (Costanzi et al., 2019; Ohgami et al., 2006). These positive and negative valences can evoke similar levels of arousal (Lang et al., 1998; Russell, 1980). This emotional arousal is known to affect various cognitive processes including salience and memory performance (Canli et al., 2000; Costanzi et al., 2019; Dolcos and Cabeza, 2002; Kensinger et al., 2006). In addition, the objects with the highest and lowest values are remembered better than the objects with intermediate values (Madan, 2013; Madan and Spetch, 2012). Given our data on habitual gaze preference for positively and negatively valued objects persists over long retention times, it is conceivable that the objects associated with positive or negative rewards induce greater emotional arousal compared than those associated with no reward, thereby generating MS. Future research will examine the relationship between the values of objects, emotions, and MS.

The next question about MS is why this component increases specifically during the retention period. Our model fit analysis showed that the weight of MS increased after 30 days of retention whereas that of RS decreased during same time. One possibility is that people tend to forget the specific values (positive or negative) of the objects over long periods of time, but still retain their importance, or magnitude. In this situation, choosing the objects with greater importance can reduce the uncertainty toward the value of objects and maximize reward gain and facilitate re-learning, as our simulation data suggests. Thus, the increase in the MS component can be interpreted as the appropriate strategy in uncertain situations. However, it should be noted that this strategy may not be adequate in every situation. In situations where the value of a bad object is extreme, choosing an object with larger magnitude can lead to critical consequences, such as death. Thus, this explanation of MS should be considered in the context of relatively moderate levels of values.

Brain substrates for motivational salience that guide habitual eye movement

The gaze preference driven by MS after long-term retention suggests specific brain areas that may process MS to guide habitual eye movement. Previous studies showed that a distinct group of dopamine neurons in the midbrain selectively processes information related to both aversive (air puff) and appetitive (liquid reward) stimuli (Matsumoto and Hikosaka, 2009). Notably, the activity of dopaminergic neurons is increased by the presentation of aversive stimuli as well as appetitive stimuli, suggesting that these dopamine neurons may send MS-related information to brain regions linked to habitual gaze. Because dopamine neurons are thought to be involved in learning and memory processing, these target structures plausibly receive MS information from the dopamine neurons. These brain regions may both learn positive and negative object values and process MS-driven habitual eye movement (Kim and Hikosaka, 2013; Matsumoto and Hikosaka, 2009).

It has been reported that caudal regions of the basal ganglia, including the ventral striatum, caudate nucleus, globus pallidus, and substantia nigra selectively represent the long-term value memory of visual objects to guide the habitual gaze preference toward positively valued objects (Kang et al., 2021; Kim and Hikosaka, 2013; Kim et al., 2017; Yasuda et al., 2012). Inactivation of the caudal part of the caudate nucleus (caudate tail) selectively impaired habitual gaze but not controlled eye movements, indicating a selective role of the caudal basal ganglia in habitual eye movement (Kim and Hikosaka, 2013). Two groups of neurons

have been found in the caudate tail: positive value-coding neurons that respond more to positively valued objects, and negative value-coding neurons that respond to the opposite information (Kim and Hikosaka, 2013). These two types of neurons are generally thought to guide positively valued object choice and negatively valued object rejection through the direct and indirect basal ganglia pathways, respectively (Amita et al., 2020; Kim et al., 2017). However, it is still possible that the positive value-coding and negative value-coding neurons together drive the habitual gaze preference for both positively valued and negatively valued objects a month after learning (Vicente et al., 2016). These positive-coding and negative-coding neurons are also found in value-coding brain regions including the orbitofrontal cortex and amygdala, possibly driving opposite and similar behaviors according to the retention period (Barberini et al., 2012).

In addition, the caudal structures in the basal ganglia receive inputs from the dopamine neurons in the midbrain region (Kim et al., 2015). However, it is not known whether these dopamine neurons processing MS information project to caudal regions in the basal ganglia related to habitual eye movement. This dopaminergic projection to the caudal basal ganglia may generate MS to drive approach responses to both positively valued and negatively valued objects automatically.

Given the possible sources of MS, what accounts for the temporal dynamics in the extent to which MS and other salience components drive habitual gaze behavior? A plausible explanation is that each salience component may be processed in different brain areas with different time courses for dynamic changes, such as different time courses for value learning in different brain regions (Morrison et al., 2011). How brain regions process each salience component is an important question for the future.

Implication of motivational salience-guided gaze behavior in re-learning after forgetting

It is natural that when the memory is vague, animals make choices based on what is best remembered to maximize the reward. A month after learning under free-viewing conditions, subjects gazed more at positively and negatively valued objects than neutral objects, suggesting that gaze was automatically decided based on the memory that was best remembered. Indeed, subjects explicitly remembered positively valued and negatively valued objects better than neutral objects after a long retention time (Figure 1F). We further demonstrated the advantage of habitual gaze based on this vague memory: Gaze preference toward objects previously associated with the highest and lowest reward values can maximize the reward gain under simulated conditions of forgetting (Figure 5C). The MS-guided gaze preference observed in this study and its advantage in simulated conditions where values are forgotten suggests how animals can efficiently maximize reward with this gaze choice strategy, even after forgetting previously learned values. Therefore, future studies with human participants will be needed to demonstrate whether MS-guided gaze preference results in this benefit in re-learning.

Our data and model indicate that dynamic changes in 3-salience components drive habitual eye movement to learned objects. However, the contribution of salience components differs depending on how ambiguous the memory of an object value is. We also demonstrate that a MS component is critical to predicting habitual gaze preference when memory decays. Our 3-salience model provides a paradigm for understanding how perceptual and cognitive salience components are organized to achieve optimal behavior when automatically selecting valuable objects.

STAR★METHODS

Detailed methods are provided in the online version of this paper and include the following:

- KEY RESOURCES TABLE
- RESOURCE AVAILABILITY
 - Lead contact
 - Materials availability
 - Data and code availability
- EXPERIMENTAL MODEL AND SUBJECT DETAILS
- METHOD DETAILS
 - Stimuli
 - Task design
 - Apparatus
 - Computing perceptual saliency during the free-viewing task

- The drift-diffusion model (DDM) for the free-viewing condition
- Model fitting
- Model evaluation
- Alternative model comparison
- Simulation
- **QUANTIFICATION AND STATISTICAL ANALYSIS**

SUPPLEMENTAL INFORMATION

Supplemental information can be found online at <https://doi.org/10.1016/j.isci.2022.105104>.

ACKNOWLEDGMENTS

This work was supported by the Neurological Disorder Research Program (NRF-2020M3E5D9079908), Korean government (MSIT) grant (NRF-2019R1A2C2005213, NRF-2019R1A6A1A10073437), and Creative-Pioneering Researchers Program through Seoul National University.

AUTHOR CONTRIBUTIONS

Methodology, S.H.H. and Y.S.R.; Investigation, S.H.H. and Y.S.R.; Visualization, S.H.H. and Y.S.R.; Supervision, H.F.K.; Writing, S.H.H., Y.S.R., S.M.P., and H.F.K.

DECLARATION OF INTERESTS

The authors declare no competing interests.

Received: January 14, 2022

Revised: May 8, 2022

Accepted: September 7, 2022

Published: October 21, 2022

REFERENCES

- Amita, H., Kim, H.F., Inoue, K.I., Takada, M., and Hikosaka, O. (2020). Optogenetic manipulation of a value-coding pathway from the primate caudate tail facilitates saccadic gaze shift. *Nat. Commun.* *11*, 1876.
- Averell, L., and Heathcote, A. (2011). The form of the forgetting curve and the fate of memories. *J. Math. Psychol.* *55*, 25–35.
- Barberini, C.L., Morrison, S.E., Saez, A., Lau, B., and Salzman, C.D. (2012). Complexity and competition in appetitive and aversive neural circuits. *Front. Neurosci.* *6*, 170.
- Berg, D.J., Boehnke, S.E., Marino, R.A., Munoz, D.P., and Itti, L. (2009). Free viewing of dynamic stimuli by humans and monkeys. *J. Vis.* *9*, 19.1–19.15.
- Caduff, D., and Timpf, S. (2008). On the assessment of landmark salience for human navigation. *Cogn. Process.* *9*, 249–267.
- Canli, T., Zhao, Z., Brewer, J., Gabrieli, J.D., and Cahill, L. (2000). Event-related activation in the human amygdala associates with later memory for individual emotional experience. *J. Neurosci.* *20*, RC99.
- Costanzi, M., Cianfanelli, B., Saraulli, D., Lasaponara, S., Doricchi, F., Cestari, V., and Rossi-Arnaud, C. (2019). The effect of emotional valence and arousal on visuo-spatial working memory: incidental emotional learning and memory for object-location. *Front. Psychol.* *10*, 2587.
- Davis, R.L., and Zhong, Y. (2017). The biology of forgetting—aperspective. *Neuron* *95*, 490–503.
- Dolcos, F., and Cabeza, R. (2002). Event-related potentials of emotional memory: encoding pleasant, unpleasant, and neutral pictures. *Cogn. Affect. Behav. Neurosci.* *2*, 252–263.
- Ebbinghaus, H. (1913). *Memory: A Contribution to Experimental Psychology* (Columbia University).
- Foulsham, T., and Underwood, G. (2008). What can saliency models predict about eye movements? Spatial and sequential aspects of fixations during encoding and recognition. *J. Vis.* *8*, 6.1–6.17.
- Ghazizadeh, A., Griggs, W., and Hikosaka, O. (2016a). Object-finding skill created by repeated reward experience. *J. Vis.* *16*, 17.
- Ghazizadeh, A., Griggs, W., and Hikosaka, O. (2016b). Ecological origins of object salience: reward, uncertainty, aversiveness, and novelty. *Front. Neurosci.* *10*, 378.
- Graybiel, A.M. (2008). Habits, rituals, and the evaluative brain. *Annu. Rev. Neurosci.* *31*, 359–387.
- Harel, J., Koch, C., and Perona, P. (2007). Graph-based Visual Saliency (NIPS).
- Hikosaka, O., Yamamoto, S., Yasuda, M., and Kim, H.F. (2013). Why skill matters. *Trends Cogn. Sci.* *17*, 434–441.
- Itti, L., and Koch, C. (2000). A saliency-based search mechanism for overt and covert shifts of visual attention. *Vision Res.* *40*, 1489–1506.
- Kang, J., Kim, H., Hwang, S.H., Han, M., Lee, S.-H., and Kim, H.F. (2021). Primate ventral striatum maintains neural representations of the value of previously rewarded objects for habitual seeking. *Nat. Commun.* *12*, 2100.
- Kensinger, E.A., Garoff-Eaton, R.J., and Schacter, D.L. (2006). Memory for specific visual details can be enhanced by negative arousing content. *J. Mem. Lang.* *54*, 99–112.
- Kim, H.F. (2021). Brain substrates for automatic retrieval of value memory in the primate basal ganglia. *Mol. Brain* *14*, 168.
- Kim, H.F., and Hikosaka, O. (2013). Distinct basal ganglia circuits controlling behaviors guided by flexible and stable values. *Neuron* *79*, 1001–1010.
- Kim, H.F., and Hikosaka, O. (2015). Parallel basal ganglia circuits for voluntary and automatic behaviour to reach rewards. *Brain* *138*, 1776–1800.
- Kim, H.F., Ghazizadeh, A., and Hikosaka, O. (2015). Dopamine neurons encoding long-term memory of object value for habitual behavior. *Cell* *163*, 1165–1175.
- Kim, H.F., Amita, H., and Hikosaka, O. (2017). Indirect pathway of caudal basal ganglia for rejection of valueless visual objects. *Neuron* *94*, 920–930.e3.

- Kumar, R.K., Garain, J., Kisku, D.R., and Sanyal, G. (2019). Guiding attention of faces through graph based visual saliency (GBVS). *Cogn. Neurodyn.* 13, 125–149.
- Land, M., Mennie, N., and Rusted, J. (1999). The roles of vision and eye movements in the control of activities of daily living. *Perception* 28, 1311–1328.
- Lang, P.J., Bradley, M.M., and Cuthbert, B.N. (1998). Emotion, motivation, and anxiety: brain mechanisms and psychophysiology. *Biol. Psychiatry* 44, 1248–1263.
- Liu, Y., Du, S., Lv, L., Lei, B., Shi, W., Tang, Y., Wang, L., and Zhong, Y. (2016). Hippocampal activation of Rac1 regulates the forgetting of object recognition memory. *Curr. Biol.* 26, 2351–2357.
- Madan, C.R. (2013). Toward a common theory for learning from reward, affect, and motivation: the SIMON framework. *Front. Syst. Neurosci.* 7, 1–6.
- Madan, C.R., and Spetch, M.L. (2012). Is the enhancement of memory due to reward driven by value or saliency? *Acta Psychol.* 139, 343–349.
- Matsumoto, M., and Hikosaka, O. (2009). Two types of dopamine neuron distinctly convey positive and negative motivational signals. *Nature* 459, 837–841.
- Miyashita, Y., Higuchi, S., Sakai, K., and Masui, N. (1991). Generation of fractal patterns for probing the visual memory. *Neurosci. Res.* 12, 307–311.
- Morrison, S.E., Saez, A., Lau, B., and Salzman, C.D. (2011). Different time courses for learning-related changes in amygdala and orbitofrontal cortex. *Neuron* 71, 1127–1140.
- Murre, J.M.J., and Dros, J. (2015). Replication and analysis of Ebbinghaus' forgetting curve. *PLoS One* 10, e0120644.
- Navalpakkam, V., Koch, C., Rangel, A., and Perona, P. (2010). Optimal reward harvesting in complex perceptual environments. *Proc. Natl. Acad. Sci. USA* 107, 5232–5237.
- Oehm, C.R., Fell, J., Baumann, C., Rosburg, T., Ludwig, E., Kessler, H., Hanslmayr, S., and Axmacher, N. (2018). Direct electrophysiological evidence for prefrontal control of hippocampal processing during voluntary forgetting. *Curr. Biol.* 28, 3016–3022.e4.
- Ohgami, Y., Kotani, Y., Tsukamoto, T., Omura, K., Inoue, Y., Aihara, Y., and Nakayama, M. (2006). Effects of monetary reward and punishment on stimulus-preceding negativity. *Psychophysiology* 43, 227–236.
- Park, J., Shimojo, E., and Shimojo, S. (2010). Roles of familiarity and novelty in visual preference judgments are segregated across object categories. *Proc. Natl. Acad. Sci. USA* 107, 14552–14555.
- Russell, J.A. (1980). A circumplex model of affect. *J. Pers. Soc. Psychol.* 39, 1161–1178.
- Schütz, A.C., Trommershäuser, J., and Gegenfurtner, K.R. (2012). Dynamic integration of information about salience and value for saccadic eye movements. *Proc. Natl. Acad. Sci. USA* 109, 7547–7552.
- Squire, L.R. (1989). On the course of forgetting in very long-term memory. *J. Exp. Psychol. Learn. Mem. Cogn.* 15, 241–245.
- Tatler, B.W., Wade, N.J., Kwan, H., Findlay, J.M., and Velichkovsky, B.M. (2010). Yabus, eye movements, and vision. *Iperception*. 1, 7–27.
- Tatler, B.W., Hayhoe, M.M., Land, M.F., and Ballard, D.H. (2011). Eye guidance in natural vision: reinterpreting saliency. *J. Vis.* 11, 5.
- Towal, R.B., Mormann, M., and Koch, C. (2013). Simultaneous modeling of visual saliency and value computation improves predictions of economic choice. *Proc. Natl. Acad. Sci. USA* 110, E3858–E3867.
- Ventura, R., Morrone, C., and Puglisi-Allegra, S. (2007). Prefrontal/accumbal catecholamine system determines motivational salience attribution to both reward and aversion-related stimuli. *Proc. Natl. Acad. Sci. USA* 104, 5181–5186.
- Vicente, A.M., Galvão-Ferreira, P., Tecuapetla, F., and Costa, R.M. (2016). Direct and indirect dorsolateral striatum pathways reinforce different action strategies. *Curr. Biol.* 26, R267–R269.
- Yamamoto, S., Kim, H.F., and Hikosaka, O. (2013). Reward value-contingent changes of visual responses in the primate caudate tail associated with a visuomotor skill. *J. Neurosci.* 33, 11227–11238.
- Yasuda, M., Yamamoto, S., and Hikosaka, O. (2012). Robust representation of stable object values in the oculomotor Basal Ganglia. *J. Neurosci.* 32, 16917–16932.
- Zajonc, R.B. (2001). Mere exposure: a gateway to the subliminal. *Curr. Dir. Psychol. Sci.* 10, 224–228.

STAR★METHODS

KEY RESOURCES TABLE

REAGENT or RESOURCE	SOURCE	IDENTIFIER
Experimental models: Organisms/strains		
Human	Seoul National University	N/A
Software and algorithms		
MATLABR2020b	MathWorks Inc.	https://www.mathworks.com/products/matlab.html
BLIP	NIH	www.cocila.net/blip
Affinity Designer	Affinity	https://affinity.serif.com/en-us/

RESOURCE AVAILABILITY

Lead contact

Further information and requests for resources and reagents should be directed to and will be fulfilled by the Lead Contact, Hyoung F. Kim (hfkim@snu.ac.kr).

Materials availability

Visual fractal stimuli used in this study are available from the [lead contact](#) on request.

Data and code availability

The original/source data are available from the [lead contact](#) on request.

EXPERIMENTAL MODEL AND SUBJECT DETAILS

Thirty healthy adults (mean age 23.1 ± 3 years; range 18–28; 13 male) participated in the experiment. Among the 30 subjects, 29 individuals visited again more than 30 days after the last learning session and performed memory retrieval tasks. Therefore, the data from 29 of the subjects were used for behavioral analyses. All subjects provided informed consent for the procedure. The experiments received approval from Seoul National University's Institutional Review Board.

METHOD DETAILS

Stimuli

We used images of fractal objects created using fractal geometry (Miyashita et al., 1991) (Figure 1B). Luminance was equalized in the images using the SHINE (Spectrum, Histogram, and Intensity Normalization and Equalization) toolbox written with MATLAB (www.mapageweb.umontreal.ca/gosselif/shine). Among 72 objects, 24 fractal objects were selected based on a behavioral attractiveness test taken by a different 10 participants (six females, four males). In this attractiveness test, the participants rated the subjective attractiveness of each object on a scale of 1–7 (1, most attractive; 7, least attractive). Objects that scored between 3.6 and 4.6 were chosen for the main experiments and randomly assigned to two different sets (12 fractal objects per set). For each set, four objects were associated with a monetary gain (positively valued; +₩100), another four objects were paired with a monetary loss (negatively valued; -₩100), and the remaining four objects were associated with neither a gain nor a loss (neutral; ₩0) in main experiments.

Task design

Object-value learning task

The object-value learning task (Learning session) was conducted on five consecutive days. In these sessions, the subjects learned the association between each object and its pre-assigned value (either positively valued, neutral, or negatively valued) (Figures 1A and 1B). Each trial started with the presentation of a white fixation square at the center, upon which the participants were required to fixate on for 300–500 ms. If the fixation was successful, two fractal objects associated with different values were simultaneously presented at a visual angle of 10° left and right of the central fixation square, respectively. The subjects selected one of the two presented objects by making a saccade. After they selected an

object, the selected object remained on the screen for 400–600 ms, followed by a feedback phase showing the outcome (gain, loss, or nothing). This object-value learning task was conducted with two object sets. For each set, all possible object pairs associated with different values were presented on the screen (96 trials in each set). The order of the object pairs was pseudo-randomized. The order of the two object sets for each subject was randomized across days.

Free-viewing condition

To investigate memory retrieval, the subjects were tested one day after four days of learning and more than 30 days after the last learning session. The interval between the last learning day and last retrieval day was 33.93 ± 1.07 days.

The free-viewing task was performed on days 1 and 5 before the learning task (Figure 1A). During each free-viewing trial a fixation square was initially presented at one of four possible locations (a visual angle of 5° to the left, right, above, and below the central point of the screen) pseudo-randomly. After 200–600 ms, nine fractal objects (three objects for each value) were simultaneously presented in a three-by-three array for 8 s (Figure 2A). The subjects were instructed to observe the nine objects freely. Each free-viewing condition consisted of 16 trials. Each three-by-three array of nine fractal objects was set before the experiment such that the number of times a specific object was presented across all 16 trials was equal. Each array contained three positively valued, three negatively valued, and three neutral objects. The order in which the 16 arrays were presented to each participant was randomized.

Explicit-memory task

In the Retrieval session, the participants went through both free-viewing conditions and the explicit memory task, which was conducted one day after the last learning session (day 6). At least 30 days after last learning, both the free-viewing session and explicit memory task were conducted, and the order of the two tasks was randomized across participants. In the explicit memory task, each object was presented with choices at the bottom (Figure 1E). The subjects were instructed to answer whether they had seen the object, and if the learned object was presented, the subjects had to choose the value of the learned object by moving the arrow with the keyboard. Among 48 fractal objects presented in the task, 24 objects were associated with value in the Learning session. Another 12 objects were from the control experiment and the other 12 objects were newly presented. We used different sets of newly presented objects on day 6 and day >30. The subjects had six choices (“+100,” “0,” “-100,” “not sure,” “new,” and “score uncertain”). If the subjects thought they knew the object value from the learning session, they were instructed to respond with the exact value of the object by choosing from “+100,” “0,” and “-100” options. However, if they thought they recognized the previously learned object but were unsure of its value, they answered with “score uncertain.” If the object was newly presented, the subjects selected “new.” If the subjects did not even know whether the object was newly presented, they chose “not sure.”

Control learning task

To rule out the possibility that gaze preference toward positively valued objects results from a higher exposure level as learning proceeds, we also conducted a control experiment with a different set of objects (Figure S2). In this experiment, the same subjects performed the control learning task. For this task, the 12 fractal objects were classified into high-, low-, and no-exposure categories. In each trial of the task, one fractal object was presented on the left or right side of the screen. The subjects were asked to make a saccade to the presented object, which remained on the screen for 400–600 ms. Each object from the high-exposure category and the low-exposure category was presented 16 times and 8 times, respectively. The objects in the no-exposure category were never presented during the control learning task. Each object appeared an equal number of times in the left and right positions on the screen.

Apparatus

Eye position data were acquired using the Oculomatic Pro 1000 eye tracker (Bio-Signal, Texas, USA) at a sampling rate of 1,000 Hz. The output of the eye tracker was recorded with a data acquisition board (PCIe-6353, National Instruments, USA) interfaced through a shielded I/O connector block (SCB-68, National Instruments, USA). The visual images were presented via a 27-inch monitor (1920 × 1080 resolution, 240 Hz refresh rate). All behavioral tasks were controlled by a custom behavior controlling system (Blip; available at www.cocila.net/blip).

Computing perceptual saliency during the free-viewing task

The perceptual saliency for each object was computed using the GBVS algorithm (Harel et al., 2007). Previous research reported that when observers view scenes presented on monitors, they tend to look more frequently to the center of their eye field than to the periphery (Foulsham and Underwood, 2008). GBVS automatically implements weights on the center of the screen to account for this central bias in fixation. However, because the initial fixation point in our task is not in the center of the screen, and our analysis requires an accurate computation of saliency for each saccade, we needed to implement weights around the fixation point before each saccade rather than the center of the screen. Therefore, we deactivated the default center bias algorithm in the GBVS and fitted the Gaussian kernel at each saccade to account for central bias in fixation as shown in

$$\text{Saliency}_{j, \text{adjusted}} = \text{Saliency}_{j, \text{pre-adjusted}} * e^{-\frac{1}{2} \left(\frac{d(x_j, x_k)}{\sigma \sqrt{2\pi}} \right)^2} \quad (\text{Equation 1})$$

where $\text{Saliency}_{j, \text{adjusted}}$ denotes the saliency value of object j with the central bias, $\text{Saliency}_{j, \text{pre-adjusted}}$ denotes the saliency value of object j computed by the GBVS, and $d(x_j, x_k)$ denotes the 2D Euclidean distance between locations of an object j and an object k before each saccade. The σ corresponds to standard deviation (SD) of the Gaussian kernel.

Thus, the same object can have different saliency values depending on the fixation point preceding each saccade. The σ was fitted to maximize Spearman's correlation coefficient between saliency rank (e.g., 1 to 9) computed from $\text{Saliency}_{j, \text{adjusted}}$ and the total number of saccades to objects corresponding to each of the nine ranks. To strictly compute perceptual saliency, we only used the data from the free-viewing condition on the first day. The MATLAB interior-point optimization algorithm was used for the fitting.

The drift-diffusion model (DDM) for the free-viewing condition

To calculate the drift rate in a drift-diffusion model, we computed the rank of three types of objects based on perceptual saliency (low, medium, and high), reward value (−100, 0, and +100), and both positive and negative values (0, and 100 from |+100| or |−100|) in ascending order to bin the object category.

Three models were examined: 1) a reward value salience model 2) a motivational salience model and 3) a 3-saliency component model (Equation 2). A weighted sum of object ranks was used to compute a_j , the drift of j^{th} accumulator (object;) as shown in Equation 2. The drift was used to compute the probability of choosing each object using the closed-form equation described in Towal et al. (2013).

$$a_j = W_{PS}R_{PS} + W_{RS}R_{RS} + W_{MS}R_{MS} \quad (\text{Equation 2})$$

where R_{PS} , R_{RS} and R_{MS} are the perceptual saliency, reward value and extreme value ranks, respectively, and W_{PS} , W_{RS} , and W_{MS} are weights to be fitted for each of the ranks.

Model fitting

To fit the DDM model to our data (Figure 3A), we first binned the data into nine groups based on R_{PS} , R_{RS} and R_{MS} . Data were binned across nine groups ($3 R_{PS} \times 3 R_{RS}$). Note that the R_{MS} does not increase the number of groups because it is contingent on the reward value rank. Consequently, we computed a frequency for each group chosen. We fitted the weights W_{PS} , W_{RS} and W_{MS} in Equation 2 to minimize the chi-square statistics (Equation 3).

$$\chi^2 = \sum_{PS,RS,MS} \frac{(O_{PS,RS,MS} - E_{PS,RS,MS})^2}{E_{PS,RS,MS}} \quad (\text{Equation 3})$$

where O denotes the observed frequency and E denotes mean expected frequency, which is computed by the expected percent chosen from the DDM \times total number of object_{PS,RS,MS} appearing on the screen.

Model evaluation

We had divided the objects into nine different categories based on PS, RS, and motivational salience levels. Model analysis of the individual subjects' data resulted in empty categories because there were cases in which the individuals did not look at every object in the free-viewing condition. Our model parameters were optimized by minimizing the chi-square difference between the expected and empirical number of

saccades to objects in each category. Therefore, the model analysis was not feasible with empty categories. To address this issue, we randomly selected five subjects and performed model fitting for 100 iterations. The training and test sets were designated to prevent the overfitting. We performed 5-fold cross validation and computed AIC statistics as shown in Equation 4. 5-fold cross validation was performed to secure sufficient data points for a test set. The AIC statistics were also used for computing model fits to divide RS and MS groups.

$$AIC = N * \ln\left(\frac{\chi^2}{N}\right) + 2K \quad (\text{Equation 4})$$

where N denotes the number of data points, χ^2 denotes the chi-square statistics, and K denotes the number of free parameters.

Alternative model comparison

Because previous studies (Ghazizadeh et al., 2016b; Madan, 2013; Madan and Spetch, 2012) demonstrated that intermediate values are more poorly retrieved than extreme values, we reasoned that the most logical alternative components should also have less weight on one of the three values than the rest. Therefore, we examined whether models with components with less weight on either the good (1:2:2) or bad (2:2:1) explains the data better than the 3SC model, in which less weight was assigned to the neutral.

Simulation

Behavioral simulation based on various choice behaviors was performed under a Bayesian belief update framework (Figure 5A). We set the classical multi-armed bandit problem with objects with deterministic reward magnitudes of $-\epsilon$, 0 and $+\epsilon$ for negatively, neutrally, and positively valued objects, respectively. We adopted deterministic objects to directly address our experimental condition. Different values of epsilon for the distributions were examined to fit the epsilon to our experimental data. Specifically, we optimized for the epsilon that minimizes the summed squared differences in percent at which subjects choose positively, neutral, and negatively valued objects on day 5. This was evaluated after the value of each object was revealed and posterior belief was updated accordingly, as frequently as the average time subjects were rewarded with each object. The simulation consisted of learning, forgetting, and re-learning phases. During the learning phase, objects were chosen based on the prior, and the values of the chosen objects were revealed. The likelihood function from the value of the chosen object was multiplied by the prior to compute posterior belief over the object's mean reward distribution.

To simulate the varying extent of forgetting, we added the forgetting factor (F) by the SD of the prior distribution. We defined complete forgetting as when the observer starts to choose positively, neutral, and negatively valued objects at levels similar to chance. Consequently, we let the observer choose positively valued, neutral, and negatively valued objects in varying forgetting conditions at a ratio specified in the choice behaviors to re-learn the distribution of each object.

Choice behaviors after forgetting consisted of four different ratios, through which observers chose positively valued, neutral, and negatively valued objects in a 2:1:2 (MS-guided choice), 2:2:1, 1:2:2 or 3:2:1 (RS-guided choice) ratio. We hypothesized that the advantages of a particular choice behavior would be apparent during the earlier phase under limited time. Therefore, we examined the first 50 re-learning steps, during which the posterior distribution was obtained by the prior updated with likelihood function at each step. To evaluate the consequences of each choice, we computed the mean reward gain. The mean reward gain was computed from 300 iterations of sampling from posterior distributions of positively, neutral, and negatively valued objects. For each iteration we assumed that the hypothetical subject would choose the object with the greatest sampled values. We computed the mean of these values across the 300 iterations and refer to it as the mean reward gain at each re-learning step. We did not update the prior during the 300 iterations of sampling to examine the efficiency of each learning strategy during the exploration. This evaluation was performed for four difference choice strategies as in Figure 5A. The sum of mean reward gain in the first 50 re-learning steps was used to compute the cumulative reward gain.

QUANTIFICATION AND STATISTICAL ANALYSIS

For examining the learning progress, repeated-measures ANOVAs were conducted to determine statistical significance of the value, day, bin, or interaction effects. The ANOVAs were followed by post hoc

Bonferroni comparisons for multiple comparisons to compare the means of the two datasets. In the t tests, if any interaction effect was revealed in the ANOVA, we used one-tailed t tests with the assumption of a predicted direction; otherwise, we used two-tailed t tests. For repeated-measures ANOVAs, we used the Greenhouse–Geisser correction if sphericity assumptions were not met. For ANOVAs on habitual behavior and model comparisons, one-way ANOVA was followed by post-hoc Bonferroni for multiple comparisons. To test the explicit memory performance and group comparison, right-tailed binomial test (based on 6 choices available) and Pearson’s rank correlation were conducted, respectively. The statistical analyses were performed using MATLAB.